Available online at www.sciencedirect.com

ScienceDirect

JOURNAL OF RARE EARTHS

ELSEVIER

JOURNAL OF RARE EARTHS, Vol. 32, No. 12, Dec. 2014, P. 1109

www.re-journal.com/en/

Photoluminescence properties of Ca-doped $BaMgAl_{10}O_{17}$:Eu^{2+},Mn^{2+} blue phosphor using BaF_2 and CaF_2 as co-flux

YE Linqin (冶林琴)[1], PENG Xingping (朋兴平)[1,*], ZHANG Shuihe (张水合)[2], WANG Yuhua (王育华)[2,*], CHANG Wenrui (常文瑞)[1]

(1. Key Laboratory for Magnetism and Magnetic Materials of the Ministry of Education, Lanzhou University, Lanzhou 730000, China; 2. Department of Materials Science, School of Physical Science and Technology, Lanzhou University, Lanzhou 730000, China)

Received 5 March 2014; revised 12 June 2014

Abstract: Ca-doped $BaMgAl_{10}O_{17}$:Eu^{2+},Mn^{2+} (BAM) blue phosphors were synthesized by flux assisted solid-state reaction method using CaF_2 and BaF_2 as co-flux. Good dispersity and particle size homogenization of hexagonal pure phase BAM were obtained by sintering at 1400 °C. The effects of the Ca^{2+} ions content on the structure, morphology and photoluminescence properties of the phosphors were studied. The results indicated that the incorporation of Ca could decrease the lattice constant, improve the homogeneity and dispersity and enhance the photoluminescence (PL) intensity of the phosphor effectively. The optimum $Ba_{0.86}Ca_{0.04}Mg_{0.97}Al_{10}O_{17}$:$0.1Eu^{2+}$,$0.03Mn^{2+}$ PL intensity was enhanced for about 30% and relative brightness was improved about 4%. Furthermore, the synthesized BAM and commercial BAM phosphors were annealed for 30 min at 600 ºC in air. The Ca-doped phosphors had stronger emission intensity, higher brightness and better chromaticity stability than that of the commercial phosphor. These results indicated that Ca-doped blue phosphors had good potential applications in the commercial tricolor fluorescent lamps as well as in other display and lamps.

Keywords: $BaMgAl_{10}O_{17}$:Eu^{2+},Mn^{2+}; BAM; CaF_2; flux; phosphor; rare earths

---

Europium-doped barium magnesium aluminates phosphor $BaMgAl_{10}O_{17}$:Eu^{2+} (BAM) is widely used as a blue phosphor in commercial applications such as tricolor fluorescent lamps (FL), light emitting diodes (LED), and plasma display panels (PDP)[1–3] because of its remarkable performance in terms of quantum efficiency, chromaticity[4], and efficient absorption of ultraviolet light. In order to improve the efficiency luminescent intensity at blue-green light area (500–530 nm)[5] of the FL, Mn^{2+} is also added during the process of the BAM blue phosphors synthesis. Nevertheless, the thermal degradation on the luminescent efficiency decline and the color coordinate offset of BAM phosphors would appear in the baking process during the FL manufacturing[6]. This degradation is a significant shortcoming in the application of BAM because of its negative influence on the longevity and quality of FL[7].

Surface coating method is usually used to solve the degradation problem. Coating the phosphor surface with fluoride or oxide such as MgF_2, SiO_2 or MgO[8–10] could avoid phosphor degradation effectively. However, the disadvantages of coating, such as nonuniformity, defective and complexity, make this method not that feasible in the industry. In recent years, several researchers reported that doped Ca^{2+}, Mg^{2+}, Si^{3+}-N^{3-} or Er^{3+}[11–14] could reduce the degradation and improve the thermal stability of the BAM phosphors, on the solid-state reaction method. However degradation is still a severe problem, which needs a solution. It is well known that BaF_2 and NH_4F[15,16] conventionally perform as flux for BAM phosphors on the solid-state reaction method. Using BaF_2 flux could reduce the sintering temperature and improve the size distribution uniformity as well as particle morphology regularity of the phosphors effectively. As far as we know, there is not yet a systemic paper report about CaF_2 used as a flux for BAM synthesis. In this work, we tried to prepare BAM with method where BaF_2 performed as component and flux, while CaF_2 acted as flux and dopant. The phosphors were also annealed 30 min at 600 ºC in air to evaluate thermal stability. The structure, morphology and PL properties of the phosphors were investigated as well.

1 Experimental

The $BaMgAlO_{17}$:Eu^{2+},Mn^{2+} were synthesized by the flux-assisted solid-state reaction method where the flux was comprised of 6.0 wt.% BaF_2 (nominal doping con-

---

Foundation item: Project supported by National Science Foundation for Distinguished Young Scholars (50925206), Gansu Provincial Science and Technology Department (041214)

* **Corresponding authors:** WANG Yuhua, PENG Xingping (**E-mail:** wyh@lzu.edu.cn, pengxp@lzu.edu.cn; **Tel.:** +86-0931-8912772, +86-0931-8912772)

DOI: 10.1016/S1002-0721(14)60190-3

tent) and 0–1.0 wt.% CaF_2 (nominal doping content). Besides, α-Al_2O_3 (AR), MgO (AR), $BaCO_3$ (AR), $MnCO_3$ (AR), and Eu_2O_3 (99.99%) were serviced as raw materials. Starting materials were uniformly mixed as stoichiometric ratio with adding suitable anhydrous ethyl alcohol. After that, the mixed precursor was sintered at 1400 ºC for 4 h in a reduction mixing gas of 5% H_2 and 95% N_2 at tube furnace. Then, the calcined phosphors were washed in pure water and then dried. The subsequent annealing processes were applied in chamber furnace at 600 ºC for 30 min in air for evaluated thermal stability. The commercial BAM was provided by Gansu Rare Earth New Material Company Limited.

The structures of phosphors were measured by a Rigaku D/Max-2400 X-ray diffractometer (XRD) with Cu Kα radiation. The morphologies of the phosphors were detected by a Hitachi &S-3400N scanning electron microscope (SEM). The comparison of phosphors properties between the non-doped and CaF_2-doped BAM was done through a Hitachi S-4800 energy dispersive spectroscope (EDS). The photoluminescence (PL) spectra were measured at room temperature by an Edinburgh FLS-920T fluorescence spectrophotometer equipped with Xe 900 as light source. The phosphors relative brightness was measured by a Hangzhou JY2003 phosphor relative Brightness meter at room temperature. The chromaticity coordinate and the central wavelength were calculated via Zolix Color Convert PR650 software.

2 Results and discussion

2.1 Structure and morphology

The XRD patterns of the phosphors with different contents of CaF_2 are depicted in Fig. 1(a). In all cases, the peaks matched well with the standard pattern of BAM (JCPDS card 26-0163, space group *P*6₃/*mmc*). The Ca-doped phosphors showed pure crystalline phase. Fig. 1(b) presents the variation of unit cell parameters of Ca-doped phosphors with different concentrations of CaF_2 flux. It was found that the unit cell parameters *a* and *c* decreased with increasing CaF_2 content, which suggests that part of doped Ca^{2+} would replace Ba^{2+} ions' sites on the host lattice of BAM:Eu^{2+},Mn^{2+}. By the way, the change trend that both parameters decreased with increasing the doped concentration was in agreement with the Vegard's law.

Fig. 2(a), (b) show the EDS spectra of sample without CaF_2 and with 0.6 wt.% (the concentration was in agreement with stoichiometric ratio 0.04 in chemical formula) CaF_2 respectively (Here, we did not show all the EDS data of our serial samples). In Fig. 2(b), there are two Ca element peaks which appear at 0.5 and 3.7 keV in the tagged EDS spectra of the 0.6 wt.% CaF_2 flux phosphors, which side witnesses that Ca^{2+} has been doped into the host lattice of BAM:Eu^{2+},Mn^{2+} phosphors. As the content of the CaF_2 flux increased, there were more Ca^{2+} ions replacing Ba^{2+} ions, and then the cell parameters *a* and *c* decreased as a result.

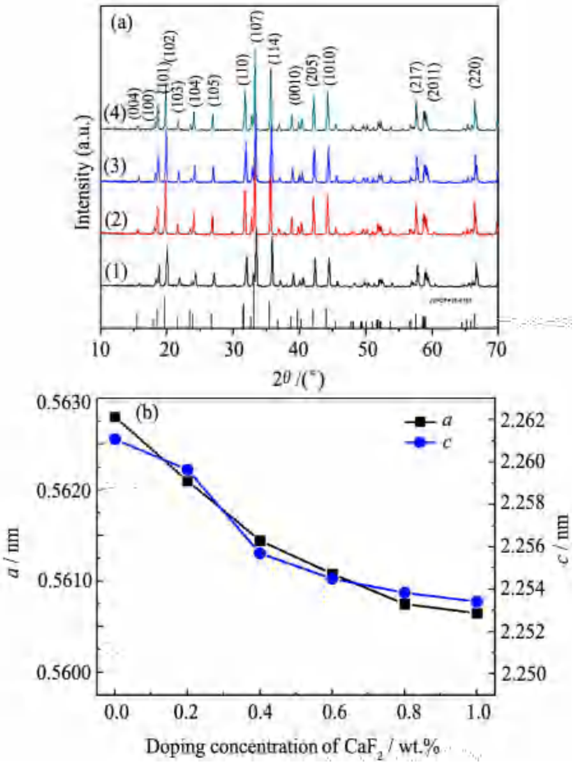

Fig. 1 (a) XRD patterns of $BaMgAl_{10}O_{17}$:Eu^{2+}, Mn^{2+} phosphors with different CaF_2 doping concentrations, 0.0 wt.% (1), 0.6 wt.% (2), 0.8 wt.% (3), 1.0 wt.% (4); (b) The dependence of unit cell parameters (*a* and *c*) of BAM phosphors on CaF_2 nominal doping concentration

The SEM morphology of BAM phosphors with different CaF_2 flux contents is provided in Fig. 3(a–f). The particles were becoming thicker with regular morphology and good dispersity when content of Ca^{2+} changed from 0.0% to 0.2%, which can be identified from the comparison between Fig. 3(a) and (b). Moreover, when we surveyed from Fig. 3(b) to (f), the particles of our samples showed gradually hexangular shape with regular profile and good dispersity, and the particle size increased by increasing the doped concentration. The granular dispersity and particle size homogenization (about 3–5 μm) slightly improved without agglomerate phenomenon aggravated when doping concentration reached to 0.6 wt.%. We found that Ca-doping improved the phosphors agglomeration and increased phosphor grains size, which was attributed to the effect of co-flux. The 0.6% doped samples manifested best morphology with particle size 3–5 μm, which can be very validly proved by the result of calculated particles distribution (the picture are not shown here). Therefore we predicted that the best luminescence characteristics would be of the d sample.

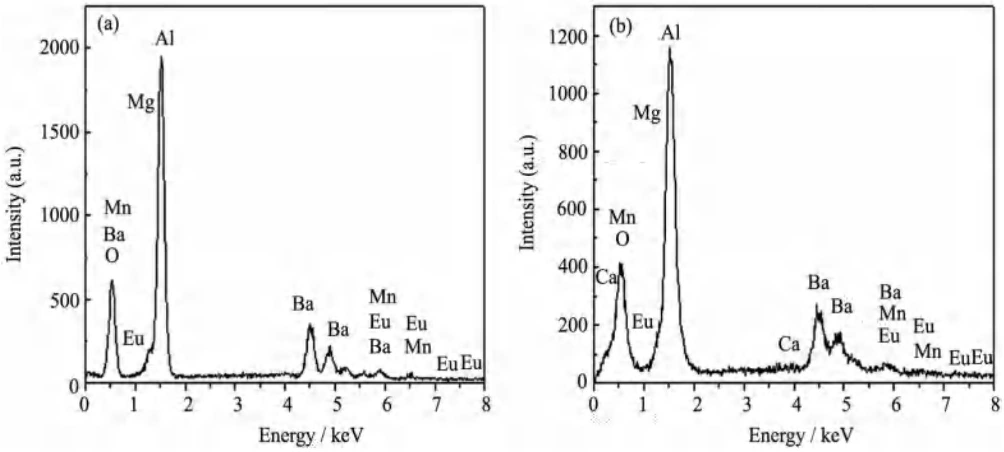

Fig. 2 (a) EDS result of phosphors without doping CaF$_2$; (b) EDS spectrum of phosphors doped with 0.6 wt.% CaF$_2$

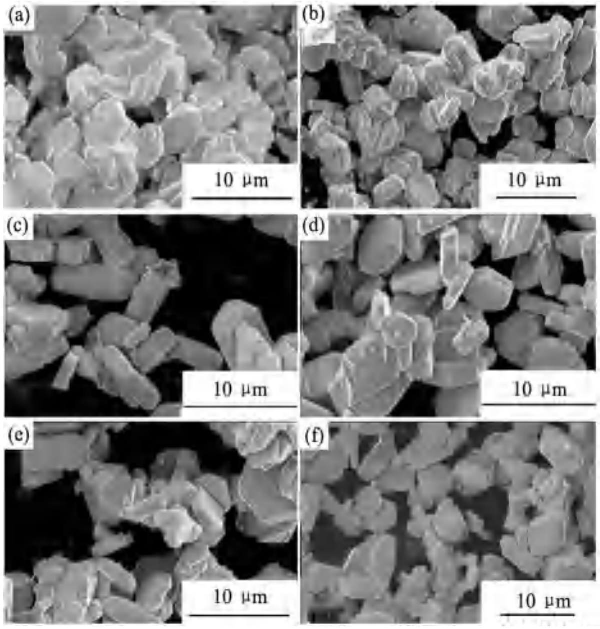

Fig. 3 SEM images of BaMgAl$_{10}$O$_{17}$:Eu^{2+},Mn^{2+} with different CaF$_2$ doping concentrations

(a) 0.0 wt.%, (b) 0.2 wt.%, (c) 0.4 wt.%, (d) 0.6 wt.%, (e) 0.8 wt.%, (f) 1.0 wt.%

2.2 Photoluminescence analysis

Fig. 4 shows the photoluminescence spectra of Ca-doped BAM phosphors with different CaF$_2$ flux contents under excitation 254 nm. There is a blue peak at ~455 nm and a green peak at ~515 nm, which originate from the Eu^{2+} 4f^{6}5d^1-4f^7 and Mn^{2+} ^{4}T$_1$→^{6}A$_1$ transition[17–19] respectively. The blue emission intensity increased with increasing the content of CaF$_2$ until up to 0.6 wt.%, and then decreased with further content increase. Experimentally, the PL intensity would increase along with the change of crystallinity and morphology. The difference of ion radius between Ca^{2+} and Ba^{2+} would decrease lattice constant, which can lead to lattice deformation in BAM structure. In the view of energy, the crystal field energy should get a perturbation when the lattice changed, which would result in the increase of luminescence efficiency. It is worthy noting that the PL maximum intensity of blue peak for 0.6 wt.% CaF$_2$ doped phosphors was about 30% higher than that of commercial phosphors, and about 4% higher for relative brightness measure. It was reported that in the conduc-

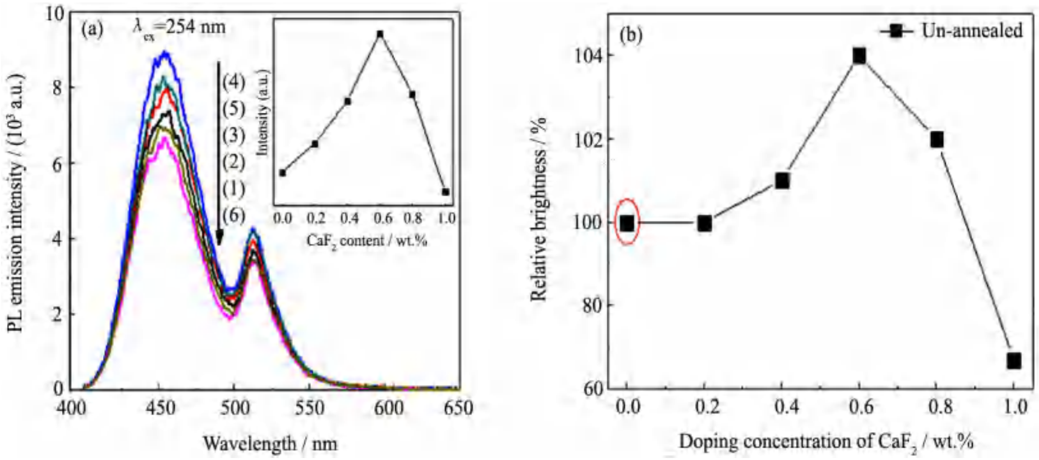

Fig. 4 (a) Photoluminescence (PL) spectra of BAM phosphors with various doping concentrations under 254 nm excitation (Numbers (1, 2, 3, 4, 5, 6) are the same represent as alphabets shown in Fig. 3, (Inset, plots of PL intensity of BAM with different doping concentrations); (b) The relative brightness curves of commercial BAM (the solid square in red circle) and different CaF$_2$-doped BAM) tion layer of the BAM, there are three prominent sites: one is Ba^{2+} substitutional Beevers Ross (BR) site and the other two interstitial sites mainly are anti Beevers Ross (a-BR) and mid-Oxygen (mO) site where Eu^{2+} would occupy[20]. More recent studies consider that the site occupancy of Eu^{2+} ions are the BR sites in BAM host lattice and the ~455 nm peak comes from the BR site Eu^{2+} $4f^65d^1$-$4f^7$ transition. The difference value between Ba^{2+} and Eu^{2+} is Δr_1 (Ba-Eu)=0.403 and that of Δr_2 (Ca-Eu)= 0.043. It is well known that ions with comparative radius can easily replace each other at lattice sites. The $\Delta r_2<\Delta r_1$ would make it easier for Eu^{2+} to replace Ca^{2+}, which means that the number of Eu^{2+} in BR sites would increase. As discussed above, doped Ca^{2+} should decrease the lattice constant as shown in Fig. 2, which would lead to the consequence that the more Eu^{2+} ions occupy the Ba^{2+} BR sites the more blue emission increases. Moreover, with the increasing content of Ca^{2+}, more Eu^{2+} ions substitute Ba^{2+} ions in the BR sites, and the PL intensity becomes stronger. However, when content of Ca^{2+} reaches 0.6 wt.%, the blue emission starts to reduce, which means critical content is encountered and we attribute it to the concentration quenching phenomenon.

In order to confirm the dependence of PL on Ca^{2+} concentration, the quantum yields of our samples also have been measured as shown in the Table 1. We found that the change of quantum yields own the similar scaling of that PL intensity performs, which indeed provides another evidence for backing the data of PL measurement.

2.3 Thermal stability analysis

The commercial and Ca-doped BAM phosphors with different CaF_2 contents were annealed at 600 ºC for 30 min in air. The PL spectra and the relative brightness variation curves of annealed phosphors are provided in Fig. 5. The blue emission intensity of Ca-doped BAM phosphors was stronger than that of commercial BAM phosphors when the content of CaF_2 flux was below 1.0 wt.%. The relative brightness of the Ca-doped BAM phosphors was higher than that of the commercial BAM phosphors. Relative brightness of the 0.6 wt.% CaF_2 Ca-doped phosphors which reached up to 98.3% of its un-annealed control was the highest in all the BAM phosphors. Here, we compared the characteristic peak in PL spectra as shown in Fig. 4(a) and 5(a) respectively. There was no obvious variation of PL spectra after annealing at 600 ºC except the intensity, which means that the characteristic peaks of Eu^{2+}/Mn^{2+} still exist without oxidization even after the annealing process at high temperature. Table 2 lists the chromaticity y-value of untreated and 600 ºC annealed BAM with different Ca-doped concentrations. Compared with the commercial phosphors, the variation of y-value of Ca-doped BAM phosphors was smaller than that of the commercial phosphors. The chromaticity of 0.6 wt.% CaF_2 flux Ca-doped phosphors was the most stable in all the BAM phosphors.

Table 1 Change of quantum yields (%) with different Ca^{2+} concentrations (wt.%)

Samples	0.0	0.2	0.4	0.6	0.8	1.0	Commercial BAM
Quantum yields	89.6	91.3	91.6	92.4	92.2	89.4	90.0

Table 2 Chromaticity y-value of untreated and 600 ºC annealed BAM with different Ca-doped concentrations (wt.%)

	Commercial BAM	0.2	0.4	0.6	0.8	1.0
Un-annealed	0.145	0.140	0.137	0.139	0.140	0.139
Annealed at 600 °C	0.134	0.136	0.135	0.138	0.138	0.134

3 Conclusions

We synthesized Ca-doped BAM blue phosphors by flux-assisted solid-state reaction method using barium source BaF_2 and calcium source CaF_2 as both component

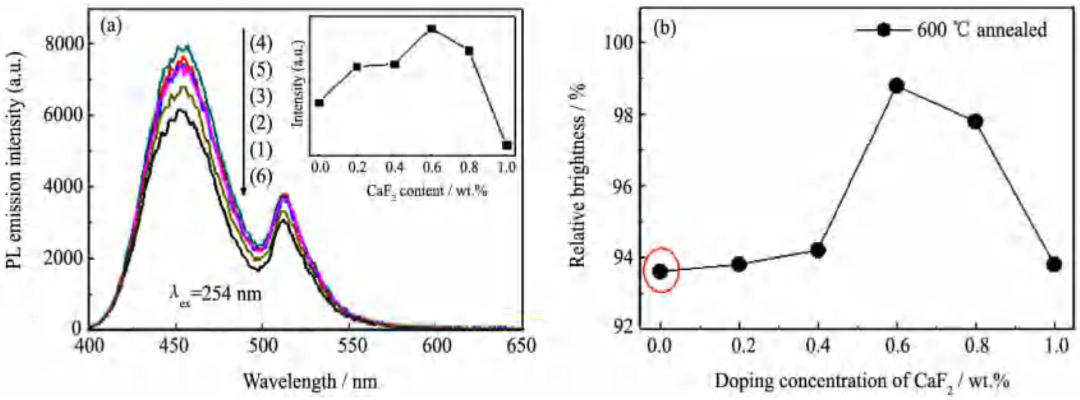

Fig. 5 (a) PL spectra of our BAM phosphors annealed at 600 °C for 30 min with different doping concentrations of CaF_2 under 254 nm excitation (Numbers 1, 2, 3, 4, 5, 6 represent the same alphabets phosphors as shown in Fig. 3. Here, the number (1) sample has the similar PL intensity with commercial BAM. The maximal peak intensity is nearby 455 nm position with different CaF_2 doping concentrations); (b) The relative brightness curves of commercial BAM (the red solid square in circle) and different CaF_2 doped BAM and co-flux, while CaF_2 as flux and dopant. The morphology of the Ca-doped BAM phosphors showed fine homogeneity and dispersity. When the content of CaF_2 was lower than 0.8 wt.%, the incorporation of Ca^{2+} ions enhanced the PL intensity and improved the brightness of BAM phosphors. After heat treatment at 600 ºC for 30 min in air, the Ca-doped BAM phosphors had stronger PL intensity, higher brightness and lower y-value variation than that of commercial phosphors. When content of CaF_2 flux was 0.6 wt.%, the Ca-doped BAM phosphors had the strongest PL intensity, highest brightness and the best thermal stability in all BAM phosphors. All these suggested that our Ca-doped blue phosphors had good potential applications in the commercial area of display and lamps.

Acknowledgements: This work was also supported by Gansu Rare Earth New Material Company Limited.

References:

[1] Wang W J, Liu B T, Wang Y H, Zhang Z Y, Chen Y S, Lan W. Morphology control and photoluminescence of $BaMgAl_{10}O_{17}$:Eu^{2+},Mn^{2+} phosphors by flux method. *Mater. Lett.*, 2011, **65**(23): 3580 .

[2] Bizarri G, Moine B. On $BaMgAl_{10}O_{17}$:Eu^{2+} phosphor degradation mechanism: ther prepared mal treatment effects. *J. Lumin.*, 2005, **113**(3): 199.

[3] Bizarri G, Moine B. On $BaMgAl_{10}O_{17}$:Eu^{2+} phosphor degradation mechanism by vacuum-ultraviolet excitation. *J. Appl. Phys.*, 2005, **98**(11): 113528.

[4] Liu B T, Wang Y H, Zhou J, Zhang F, Wang Z F. The eduction of Eu^{3+} to Eu^{2+} in $BaMgAl_{10}O_{17}$:Eu^{2+} and the photoluminescence properties of $BaMgAl_{10}O_{17}$:Eu^{2+} phosphor. *J. Appl. Phys.*, 2009, **106**(5): 053102.

[5] Justel T, Lade H, Mayr W, Meijerink A, Wiechert D U. Thermoluminescence spectroscopy of Eu^{2+} and Mn^{2+} doped $BaMgAl_{10}O_{17}$. *J. Lumin.*, 2003, **101**(3): 195.

[6] Wang Y F, Xu X, Yin L J, Lu Y H. High thermal stability and photoluminescence of Si–N-Codoped $BaMgAl_{10}O_{17}$:Eu^{2+} phosphors. *J. Am. Ceram. Soc.*, 2010, **93**(6): 1534.

[7] Tannoa H, Zhang S X, Shinod T, Kajiyam H. Characteristics of photoluminescence, thermoluminescence and thmalde gradation in Eu-doped $BaMgAl_{10}O_{17}$ and $SrMgAl_{10}O_{17}$. *J. Lumin.*, 2010, **130**(1): 82.

[8] Chen Z, Yan Y W, Liu J M, Yin Y, Wen H M, Liao G H, Wu C L, Zao J Q, Liu D H, Tian H M, Zhang C S, Li S D. Microstructure and luminescence of surface-coated nano-$BaMgAl_{10}O_{17}$:Eu^{2+} blue phosphor. *J. Alloys Compd.*, 2009, **478**(1-2): 679.

[9] Zhu P F, Zhu Q R, Zhu H Y, Zhao H F, Chen B J, Zhang Y L, Wang X J, Di W H. Effect of SiO_2 coating on photoluminescence and thermal stability of $BaMgAl_{10}O_{17}$:Eu^{2+} under VUV and UV excitation. *Opt. Mater.*, 2008, **30**(6): 930.

[10] Kuo K T, Lee S P, Chen S Y, Cheng B M, Lu H C, Liu D M, Ting C C. $BaMgAl_{10}O_{17}$:Eu blue phosphors with MgO coating and microwave irradiation. *J. Phys. Chem. Solids.*, 2008, **69**(2-3): 446.

[11] Sohn K S, Kim S S, Park H D. Luminescence quenching in thermally-treated barium magnesium aluminate phosphor. *Appl. Phys. Lett.*, 2002, **81**(10): 1759.

[12] Zhuang W D, Cui X Z, Yu Z J, Zhao C L, He H Q, Huang X W. Influence of doping on the crystal structures and luminescent properties of aluminate phosphors for plasma display panel. *Society for Information Display*, 2003, **34**(1): 1223.

[13] Wang Y F, Zhu Q Q, Hao L Y, Xu X, Xie R J, Agathopoulos S. Luminescence and structural properties of high stable Si–N-doped $BaMgAl_{10}O_{17}$:Eu^{2+} phosphors synthesized by a mechanochemical activation route. *J. Am. Ceram. Soc.*, 2013, **96**(8): 2562.

[14] Zhang J Y, Zhang Z T, Tang Z L, Tao Y, Long X. Luminescent properties of the $BaMgAl_{10}O_{17}$:Eu^{2+}, M^{3+} (M=Nd, Er) phosphor in the VUV region. *Chem. Mater.*, 2002, **14**(7): 3005.

[15] Lee S H, Koo H Y, Jung D S, Yi J H, Kang Y C. Fine-sized $BaMgAl_{10}O_{17}$:Eu^{2+} phosphor powders prepared by spray pyrolysis from the spray solution with BaF_2 flux. *Ceram. Int.*, 2009, **35**(7): 2651.

[16] Lee S H, Koo H Y, Kim J H, Ko Y N, Yi J H, Kang Y C, Lee H M, Yun J Y. $BaMgAl_{10}O_{17}$:Eu^{2+} phosphor powders prepared from precursor powders with a hollow and thin wall structure containing NH_4F flux. *Electron. Mater. Lett.*, 2010, **6**(2): 81.

[17] Zhang Z, Wang Y. Enhanced emission and improved thermal stability of $BaMgAl_{10}O_{17}$:Eu^{2+} phosphor via additional Mg^{2+} doping. *Mater. Lett.*, 2007, **61**(19-20): 4128.

[18] Jung K Y, Lee H W, Kang Y C, Park S B, Yang Y S. Luminescent properties of (Ba,Sr)$MgAl_{10}O_{17}$:Mn,Eu green phosphor prepared by spray pyrolysis under VUV excitation. *Chem. Mater.*, 2005, **17**(10): 2729.

[19] Huang S, Wei X T, Chen Y H, Yin M. Luminescence properties of a single-host phosphor $Ba_{1.8-w}Sr_wLi_{0.4}SiO_4$:$Ce^{3+}$,$Eu^{2+}$,$Mn^{2+}$ for WLED. *J. Rare Earths*, 2013, **31**(3): 227.

[20] Zhu P F, Di W H, Zhu Q R, Chen B J, Zhu H Y, Zhao H F, Yang Y J, Wang X J. Luminescent properties and thermal stability of $BaMgAl_{10}O_{17}$:Eu^{2+} synthesized by sol-gel route. *J. Alloys Compd.*, 2008, **454**(1-2): 245.